

## Original Article

# Lesions in White Matter in Wilson's Disease and Correlation with Clinical Characteristics

Anqin Wang<sup>1</sup> , Taohua Wei<sup>1</sup>, Hongli Wu<sup>2</sup>, Yulong Yang<sup>2</sup>, Yufeng Ding<sup>2</sup>, Yi Wang<sup>2</sup>, Chuanfeng Zhang<sup>1</sup> and Wenming Yang<sup>1</sup>

<sup>1</sup>The First Affiliated Hospital of Anhui University of Chinese Medicine, Hefei, Anhui 230601, China and <sup>2</sup>Anhui University of Chinese Medicine, Hefei, Anhui 230601, China

**ABSTRACT: Background:** Neuroimaging studies in Wilson's disease (WD) have identified various alterations in white matter (WM) microstructural organization. However, it remains unclear whether these alterations are localized to specific regions of fiber tracts, and what diagnostic value they might have. The purpose of this study is to explore the spatial profile of WM abnormalities along defined fiber tracts in WD and its clinical relevance. **Methods:** Ninety-nine patients with WD (62 men and 37 women) and 91 age- and sex-matched controls (59 men and 32 women) were recruited to take part in experiments of diffusion-weighted imaging with 64 gradient vectors. The data were calculated by FMRIB Software Library (FSL) software and Automated Fiber Quantification (AFQ) software. After registration, patient groups and normal groups were compared by Mann–Whitney U test analysis. **Results:** Compared with the controls, the patients with WD showed widespread fractional anisotropy reduction and mean diffusivity, radial diffusivity elevation of identified fiber tracts. Significant correlations between diffusion tensor imaging (DTI) parameters and the neurological Unified Wilson's Disease Rating Scale (UWDRS-N), serum ceruloplasmin, and 24-h urinary copper excretion were found. **Conclusions:** The present study has provided evidence that the metrics of DTI could be utilized as a potential biomarker of neuropathological symptoms in WD. Damage to the microstructure of callosum forceps and corticospinal tract may be involved in the pathophysiological process of neurological symptoms in WD patients, such as gait and balance disturbances, involuntary movements, dysphagia, and autonomic dysfunction.

**RÉSUMÉ : Lésions de la substance blanche dans le cas de la maladie de Wilson et corrélation avec des caractéristiques cliniques. Contexte :** Les études de neuro-imagerie dans le contexte de la maladie de Wilson (MW) ont identifié diverses altérations de l'organisation microstructurale de la substance blanche. Cela dit, il n'est pas clair si ces altérations sont localisées dans des régions spécifiques des faisceaux de fibres (*fiber tracts*) et quelle valeur diagnostique elles pourraient avoir. L'objectif de cette étude est donc d'explorer le profil spatial des anomalies de la substance blanche le long des faisceaux de fibres définis dans la MW ainsi que leur pertinence clinique. **Méthodes :** Au total, 99 patients atteints de la MW (62 hommes, 37 femmes) et 91 témoins appariés en fonction de l'âge et du sexe (59 hommes et 32 femmes) ont été recrutés pour participer à des expériences d'imagerie pondérée par diffusion avec 64 vecteurs de gradient. Nos données ont ensuite été calculées au moyen du logiciel *FMRIB Software Library* (FSL) et d'un logiciel de quantification automatique des faisceaux de fibres. Après l'enregistrement de ces données, les patients et les témoins ont été comparés entre eux à l'aide de l'analyse du test U de Mann-Whitney. **Résultats :** Si on les compare aux témoins, les patients atteints de la MW ont montré une réduction généralisée de l'anisotropie fractionnelle (AF) ainsi qu'une augmentation de la diffusivité moyenne (DM) et de la diffusivité radiale (DR) des faisceaux de fibres identifiés. En outre, des corrélations significatives entre les paramètres d'imagerie du tenseur de diffusion (ITD) et l'échelle neurologique unifiée d'évaluation de la maladie de Wilson, la céruloplasmine sérique (SC) et l'excrétion urinaire de cuivre sur 24 heures (EUC sur 24 heures) ont été notées. **Conclusions :** La présente étude a donc fourni des preuves que les paramètres d'ITD pouvaient être utilisés comme biomarqueur potentiel des symptômes neuro-pathologiques de la MW. Les dommages causés à la microstructure des forceps du corps calleux (CC) et du faisceau pyramidal (FP) peuvent être impliqués dans le processus physiopathologique des symptômes neurologiques chez des patients atteints de la MW, par exemple les troubles de la marche et de l'équilibre, les mouvements involontaires, la dysphagie et le dysfonctionnement autonome.

**Keywords:** Wilson's disease; Neuroradiology; Neuroimaging; Neurodegenerative disorders; Movement disorders

(Received 15 June 2022; final revisions submitted 29 July 2022; date of acceptance 3 August 2022; First Published online 12 August 2022)

## Introduction

Wilson's disease (WD) is an inherited autosomal recessive disorder due to ATP7B gene mutation, resulting in defective copper metabolism and excessive copper accumulation in the brain and

liver.<sup>1</sup> The clinical phenotype is variable, including movement disorders (ataxia and dystonia),<sup>2</sup> cognitive impairment,<sup>3</sup> depression, and generalized epilepsy.<sup>4</sup> Pharmacological therapy with anti-copper drugs is currently the main treatment method for patients with

**Corresponding author:** Wenming Yang, The First Affiliated Hospital of Anhui University of Chinese Medicine, Hefei, Anhui, 230601, China. Email: yangwm8810@126.com

**Cite this article:** Wang A, Wei T, Wu H, Yang Y, Ding Y, Wang Y, Zhang C, and Yang W. (2023) Lesions in White Matter in Wilson's Disease and Correlation with Clinical Characteristics. *The Canadian Journal of Neurological Sciences* 50: 710–718, <https://doi.org/10.1017/cjn.2022.286>

© The Author(s), 2022. Published by Cambridge University Press on behalf of Canadian Neurological Sciences Federation.

**Table 1:** Clinical and biochemical characteristics of patients with WD

At initial presentation	Patients of WD	Controls
Patients (NO.)	99	91
Males/females (NO.)	62/37	59/32
Ages (years, mean $\pm$ SD)	27.48 $\pm$ 7.34	26.01 $\pm$ 5.47
UWDRS-N score	9.22 $\pm$ 12.57	/
24-h urinary excretion of copper ( $\mu$ mol/L)	855.56 $\pm$ 592.41	/
Serum ceruloplasmin (g/L)	0.05 $\pm$ 0.04	/

WD, and most patients correctly treated respond well.<sup>5</sup> However, the neuropathological mechanisms in patients with neurological manifestations are still unclear, and neurological symptoms persist or even exacerbate.

Histopathological changes in WD have been described, including reactive astrogliosis, demyelination, central pontine myelinolysis, cavitation, and gray matter and white matter (WM) were both affected.<sup>6,7</sup> As a noninvasive tool, diffusion tensor imaging (DTI) observes water diffusion properties in the brain to reveal the histological features of WM. The metrics of DTI which reflect the condition of axons and myelin include fractional anisotropy (FA), mean diffusivity (MD), axial diffusivity (AD), and radial diffusivity (RD). Various alterations in WM microstructural organization have been identified in WD using DTI techniques.<sup>8,9</sup> However, previous DTI studies have only investigated changes in diffusion measurements of WM, and the categoric location of WM fiber bundle abnormalities remains unclear. Automated fiber-tract quantification (AFQ) can quantify the diffusion characteristics of fiber bundles along with multiple nodes point by point, instead of the average value of the entire fiber bundle, providing effective evidence for the abnormal position of fiber bundles.<sup>10</sup> AFQ has been used to study microstructural changes in a variety of neurogenic diseases and shows advantages in processing large amounts of data efficiently.<sup>11,12</sup> Deng and colleagues had introduced the AFQ method to investigate the impairment and reorganization patterns and characteristics of language-related WM in AVMs located in different brain areas.<sup>12</sup> AFQ was also used to study the disruption of WM tracts in a pointwise analysis in patients with trigeminal neuralgia.<sup>13</sup>

In this study, AFQ was applied to assess the reproducibility and diagnostic value of microstructural WM in WD patients compared with normal controls. The first goal of our study was to demonstrate the alterations in WM characteristics and the explicit location of WM fiber tract abnormalities in patients with WD. The second goal was to reveal whether abnormal WM integrity correlates with clinical severity in individuals with neuropathic WD.

## Methods

### Subjects

From April 2021 until August 2021, 99 patients with WD (62 men, 37 women; age, 27.48  $\pm$  7.34 years; age range: 17–47 years) and 91 age- and sex-matched controls (59 men, 32 women; age, 26.01  $\pm$  5.47 years; age range: 17–45 years) were recruited to participate in this study. The diagnosis of WD is based on the clinical extrapyramidal symptom and behavioral problems, Kayser-Fleischer ring, low serum copper, decreased level of serum

ceruloplasmin (SC), and increased 24-h urinary copper (24-h UC) excretion.<sup>14–15</sup> Participants with WD were censored with the Unified Wilson's Disease Rating Scale (UWDRS) score,<sup>16</sup> and the neurological examination (UWDRS-N) score, SC, and 24-h UC excretion were recorded. This study was approved by the local ethical committee, and informed consent for participation was signed. All subjects were right-handed. Detailed information regarding the subjects is presented in Table 1.

### Image Acquisition and Image Analysis

All participants were scanned on a clinical 3.0-T MR imaging system (Discovery MR750, GE Healthcare, Milwaukee, WI, USA) equipped with an eight-channel high-resolution radiofrequency head matrix coil. Sequences of imaging included T1-3D BRAVO and DTI. DTI images were acquired with the parameters as: TR/TE, 4800 ms/minimum; matrix, 128  $\times$  128; FOV, 256  $\times$  256 mm; slice thickness, 3 mm with no gap; 50 axial slices; 64 directions at a *b* value of 1000 sec/mm<sup>2</sup>; and 5 non-weighted diffusion images (*b* = 0 sec/mm<sup>2</sup>). T1-3D BRAVO images were obtained with: TR/TE, 8.2 ms/3.2 ms; FA, 12°; matrix, 256  $\times$  256; FOV, 256  $\times$  256 mm; slice thickness, 1 mm with no gap; and 166 slices.

The DTI data preprocessing was performed using Software Library (FSL version 5.0; [HTTPS://www.fmrib.ox.ac.uk/fsl/](https://www.fmrib.ox.ac.uk/fsl/)). Preprocessing steps for DTI data included image correction for motion, eddy current deformations, skull stripping, and tensor fitting with the tool of diffusion toolbox (FDT) and brain extraction tool (BET). Whole-brain diffusion metrics, including FA, MD, AD, and RD, were calculated by the DTIFIT program at each voxel. Dt6 file was obtained by T1 image aligned to raw B0 with the AC–PC plane for further analysis, and images that failed to align were culled based on the visual evaluation. Then, 20 major fiber tracts of the whole brain were identified using the AFQ toolkit (<https://github.com/yeatmanlab/AFQ>, version 1.2).<sup>17</sup> A brief description of the steps for AFQ is as follows: (1) whole-brain deterministic tractography with thresholds of turning angle <30° and FA >0.2; (2) fiber tract segmented using regions of interest (ROIs); (3) the identified fiber tract refinement based on the fiber tract probability maps; (4) fiber tract cleaning by an outlier rejection algorithm; and (5) calculation of the diffusion metrics along each fiber tract at 100 equidistant nodes. However, some fibers failed to track because of the data quality and strict criteria for tract identification. All 20 fiber bundles for each subject could not be recognized, especially the bilateral cingulum hippocampus. Thus, subjects with no more than 16 fiber bundles recognized were culled from the further analysis.

### Statistical Analysis

All statistical analyses were conducted with Statistical Package for Social Science software (SPSS, v20.0, Chicago, IL, USA). T tests and  $\chi^2$  tests were used to investigate the age and sex difference. Mann-Whitney U test was conducted in group-level pointwise analyses of the diffusion metrics across 100 points of each fiber tract, and mean values were plotted. Spearman's correlation analysis was used to assess the correlations of diffusion metrics with symptom scores, including UWDRS-N score, SC, and 24-h UC excretion, with a 0.05 significance level adopted. Square root transformation was applied to the UWDRS-N score because of its heavy-tailed shape.<sup>18</sup>

## Results

The demographic and clinical characteristics of the WD patients and controls are summarized in Table 1. There were no differences

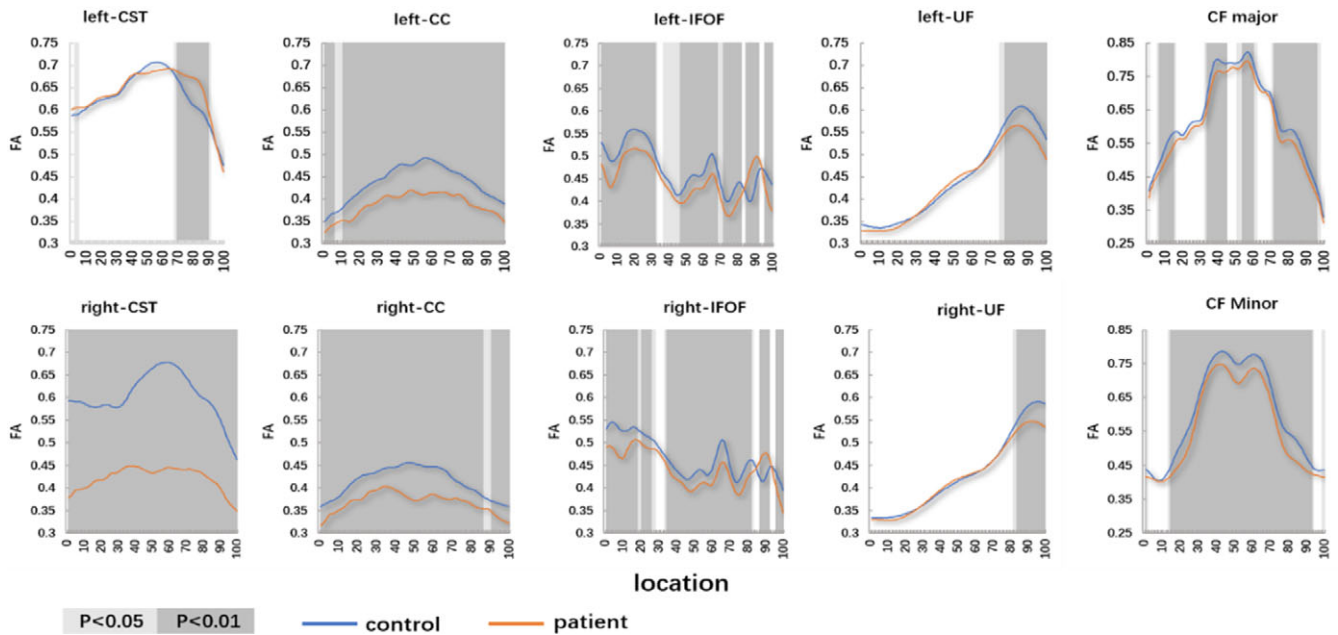


**Figure 1:** The pointwise comparison of FA profiles along the 10 fiber tracts among patients with WD and controls. Shaded gray background indicates a tract segment where the mean diffusion properties of the patients are significantly different with  $p < 0.05$  and  $p < 0.01$ .

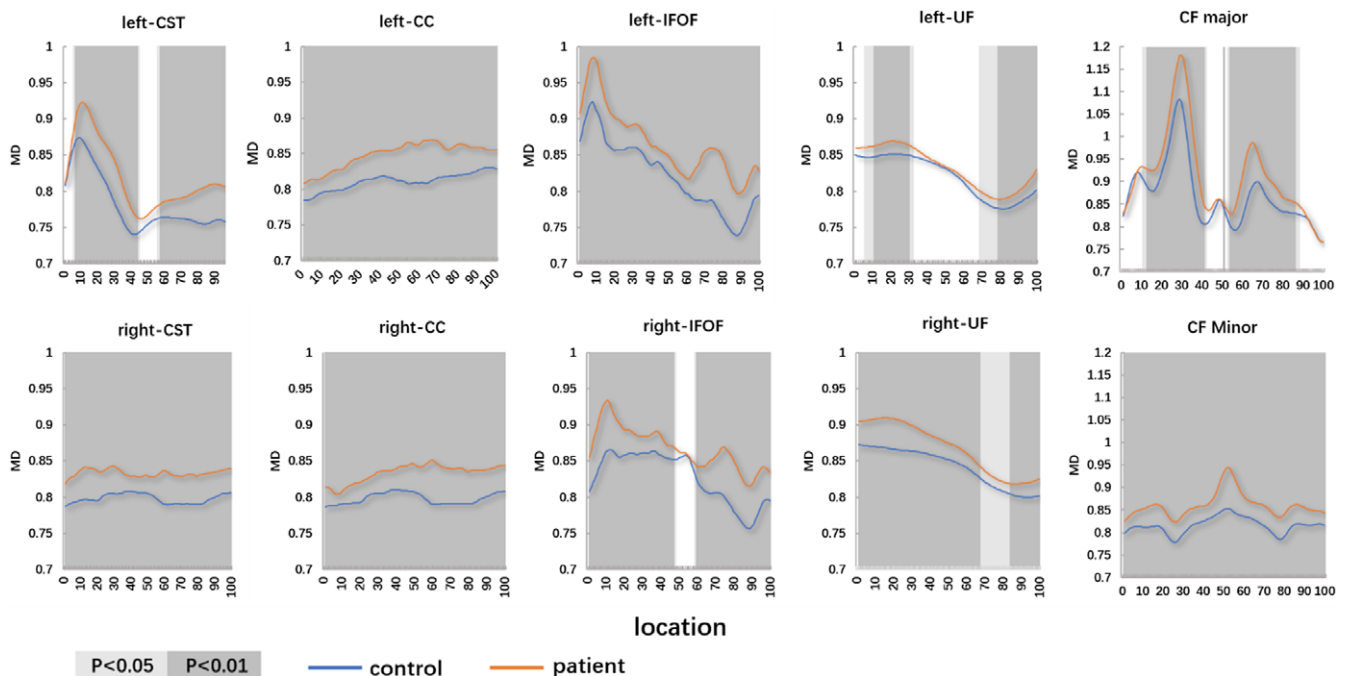


**Figure 2:** The pointwise comparison of MD profiles along the 10 fiber tracts among patients with WD and controls. Shaded gray background indicates a tract segment where the mean diffusion properties of the patients are significantly different with  $p < 0.05$  and  $p < 0.01$ .

in age and gender distribution between healthy control and patient groups.

### Diffusion Measures Changes in WD Patients

Compared with the controls, the patients with WD showed widespread FA reduction and MD, and RD elevation of identified fiber tracts. The details are as follows: (1) patients with WD showed lower mean FA values in the R-corticospinal tract (R-CST),

bilateral cingulum cingulate (CC), bilateral inferior fronto-occipital fasciculus (IFOF) (anterior and middle parts), bilateral uncinate fasciculus (UF) (posterior part), callosum forceps (CF) Major (posterior part), CF Minor and high mean FA values in the L-CST (posterior part), and bilateral IFOF (posterior part) (Figure 1). (2) Patients with WD showed high mean MD values in the bilateral CST, bilateral CC, bilateral IFOF, bilateral UF (posterior part), CF Major (posterior part), and CF Minor (Figure 2). (3) Patients with WD showed high mean AD values

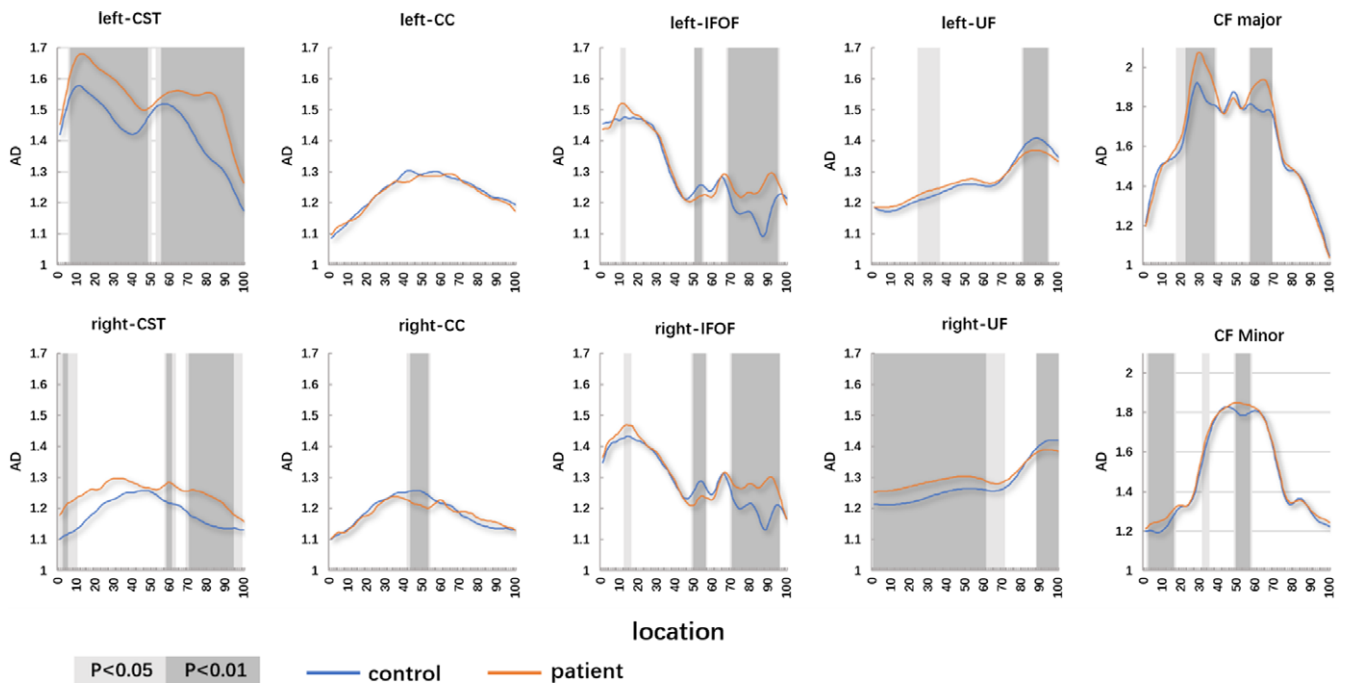


**Figure 3:** The pointwise comparison of AD profiles along the 10 fiber tracts among patients with WD and controls. Shaded gray background indicates a tract segment where the mean diffusion properties of the patients are significantly different with  $p < 0.05$  and  $p < 0.01$ .

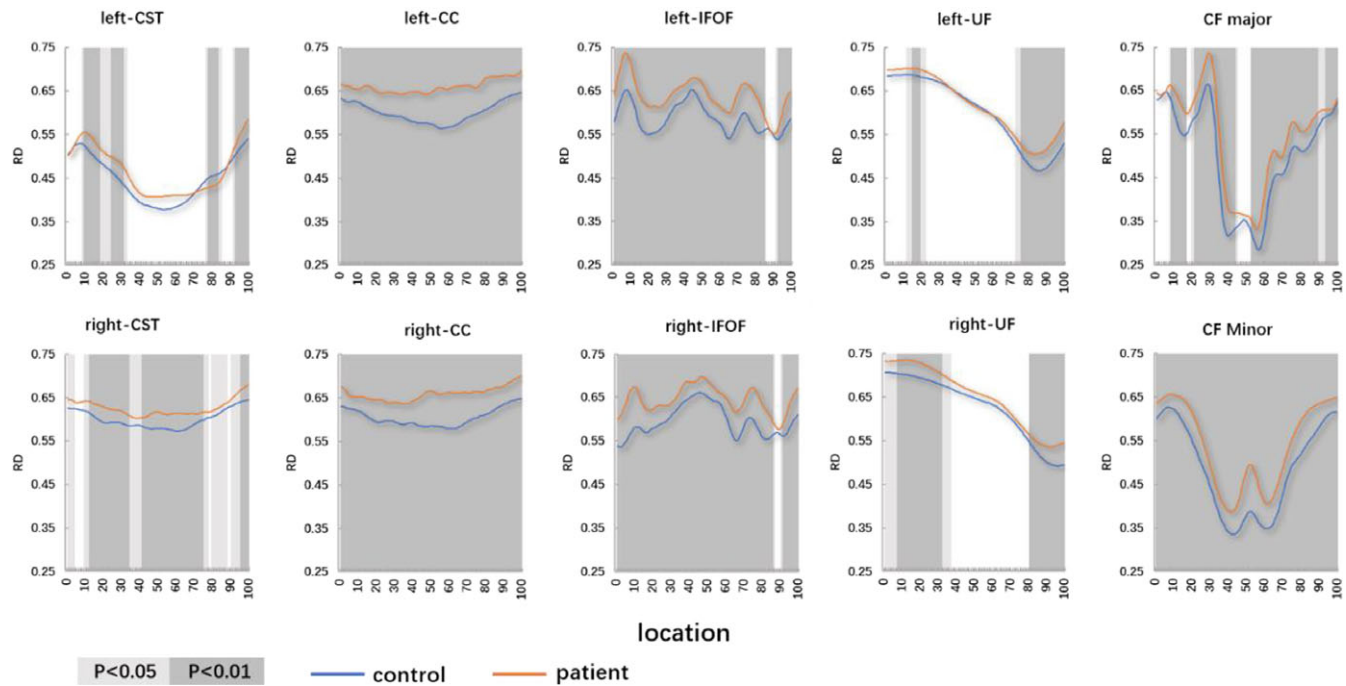


**Figure 4:** The pointwise comparison of RD profiles along the 10 fiber tracts among patients with WD and controls. Shaded gray background indicates a tract segment where the mean diffusion properties of the patients are significantly different with  $p < 0.05$  and  $p < 0.01$ .

in the L-CST (posterior part), L-IFOF (posterior part), and R-IFOF (posterior part) (Figure 3). (4) Patients with WD showed high mean RD values in the R-CST, bilateral CC, bilateral IFOF, bilateral UF (posterior part), CF Major (posterior part), and CF Minor (Figure 4). The main changes in the FA, MD, AD, and RD values of WD patients are summarized in Table 2.

### Correlation Between the Diffusion Measure and Clinical Features

Significant correlations between DTI parameters and the UWDRS-N score, SC, and 24-h UC excretion were found. The FA values in the R-CST and L-CC were negatively correlated with the UWDRS-N score ( $r = -0.36, p < 0.05$ ;  $r = -0.38, p < 0.05$ )

**Table 2:** Lesions of the main fiber

Fascicles	FA	MD	AD	RD	Impairment or remodeling	Location
L-CST (posterior part)	↑	↑	↑	/	Remodeling	Axon
R-CST	↓	↑	/	↑	Impairment	Myelin
L-CC	↓	↑	/	↑	Impairment	Myelin
R-CC	↓	↑	/	↑	Impairment	Myelin
L-IFOF (anterior and middle parts)	↓	↑	/	↑	Impairment	Myelin
L-IFOF (posterior part)	↑	↑	↑	↑	Remodeling	Axon and Myelin
R-IFOF (anterior and middle parts)	↓	↑	/	↑	Impairment	Myelin
R-IFOF (posterior part)	↑	↑	↑	↑	Remodeling	Axon and Myelin
L-UF (posterior part)	↓	↑	/	↑	Impairment	Myelin
R-UF (posterior part)	↓	↑	/	↑	Impairment	Myelin
CF Major (posterior part)	↓	↑	/	↑	Impairment	Myelin
CF Minor	↓	↑	/	↑	Impairment	Myelin

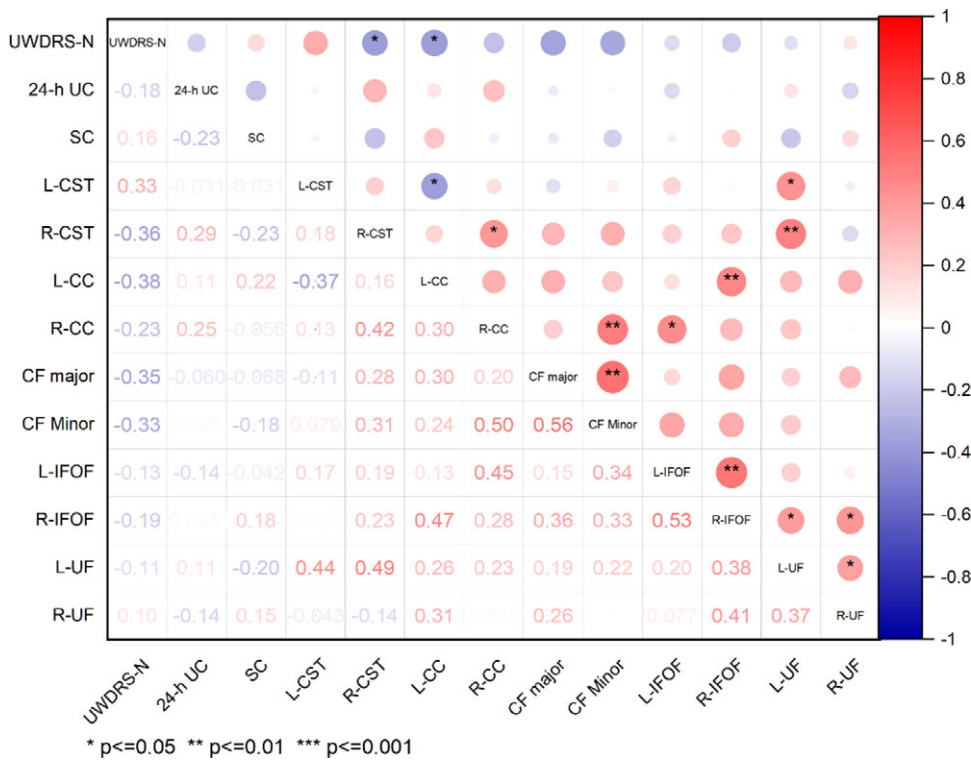


**Figure 5:** Correlation analysis between FA of fiber tracts and clinical features. Results of correlation analysis are presented as a correlation coefficient matrix. Positive correlations are shown in red, and negative correlations are shown in blue.

(Figure 5). The MD value in the L-CC was negatively correlated with the UWDRS-N score ( $r = 0.25, p < 0.05$ ) (Figure 6). There is no significant difference in the correlation between AD values and symptom scores (Figure 7). The RD values in the CF Major, CF Minor, L-IFOF, and R-IFOF were positively correlated with the UWDRS-N score, and RD values in the L-CC and L-UF were positively correlated with the SC (Figure 8).

**Discussion**

Most previous studies have focused on gray matter in patients of WD, atrophy or functional reorganization of the basal ganglia (caudate, putamen, and globus pallidus), thalamus, and red

nucleus.<sup>19,20</sup> The changes in patients with WD in the WM integrity were confirmed in previous studies.<sup>3,21</sup> As a new algorithm, AFQ reconstructs tract profiles of WM automatically and quantifies the diffusion properties at multiple nodes along the fiber tract pointwise, improving the detailed level of the analysis.<sup>22</sup> Diffusion properties (FA, MD, AD, and RD) were extracted for 100 anatomically locations. The characteristics of diffusion properties might be used as diagnostic biomarkers in these diseases of different pathologies. FA is a scalar value representing anisotropic water diffusion, which is associated with the cellular and axonal boundaries that delineate intact WM fibers; low FA values may indicate loss of WM integrity and high FA values may reflect fiber bundle plasticity.<sup>12</sup> MD represents the mean water diffusion rate, and high MD values may

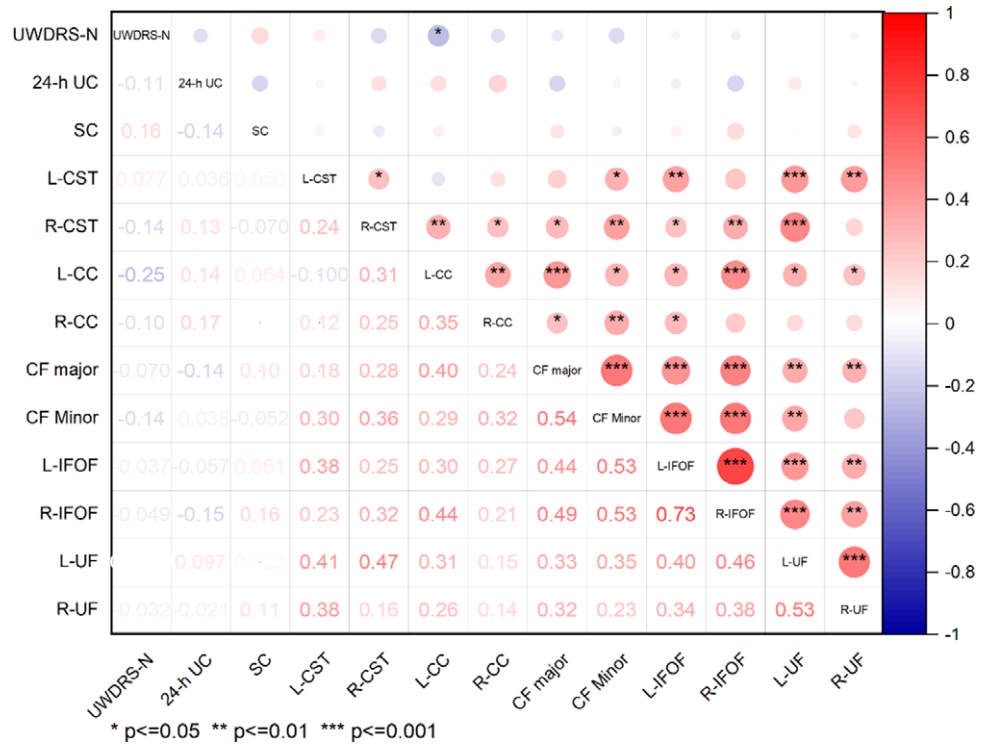


**Figure 6:** Correlation analysis between MD of fiber tracts and clinical features. Results of correlation coefficient matrix. Positive correlations are shown in red, and negative correlations are shown in blue.

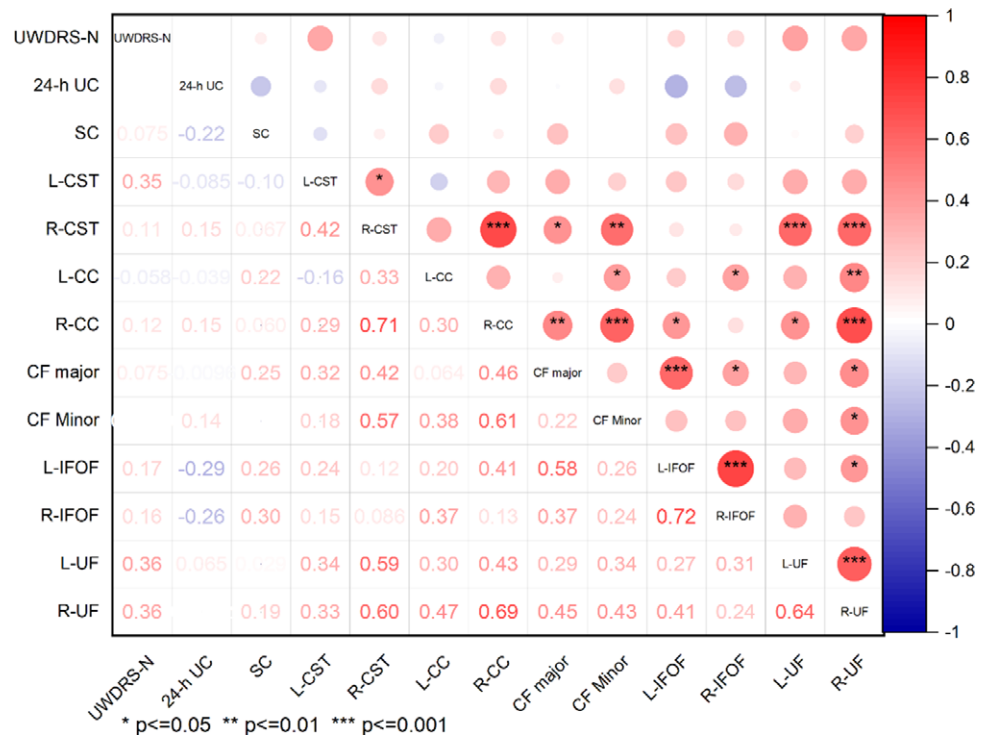


**Figure 7:** Correlation analysis between AD of fiber tracts and clinical features. Results of correlation coefficient matrix. Positive correlations are shown in red, and negative correlations are shown in blue.

indicate axonal loss and demyelination. AD describes water diffusivity along the axonal fibers, which is related to axon integrity. RD represents an average of water diffusivities perpendicular to the axonal fibers and provides information on myelination. A high RD level is associated with tract demyelination, and a low RD level may be associated with myelin reorganization.<sup>23</sup> To our best knowledge, this is the first study to explore potential regional

WM fiber alterations and WM microstructural integrity in WD patients with the AFQ technique.

In this study, MD increased in the bilateral CST, FA, and RD increased in R-CST, and FA and AD increased in L-CST (posterior part). Besides, FA values in R-CST and L-CC showed a positive correlation with UWDRS-N score. It was suggested that the neurological severity grade of WD correlated with urinary Cu.<sup>24</sup>

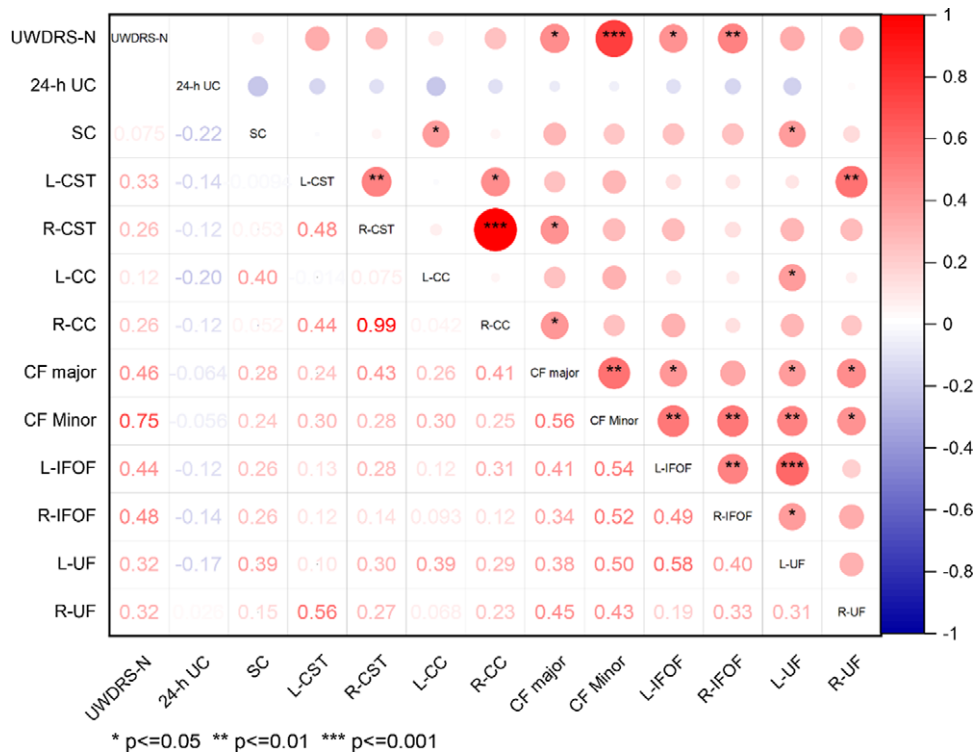


**Figure 8:** Correlation analysis between RD of fiber tracts and clinical features. Results of correlation analysis are presented as a correlation coefficient matrix. Positive correlations are shown in red, and negative correlations are shown in blue.

As a motor pathway, the CST controls the movements of the limbs and trunk, originated from the motor regions and somatosensory, and terminates at motor neurons and spinal cord interneurons.<sup>25</sup> Previous studies about structural brain imaging have demonstrated that the integrity of the CST relates to residual motor outcomes.<sup>26,27</sup> Vuong and colleagues provided preliminary evidence that there was a sensitive clinical correlate of motor and whole-brain WM tract (including the CST and CC) impairment in children with spastic bilateral cerebral palsy, suggesting that anisotropy and myelination in these regions were associated with those selective voluntary motor control.<sup>28</sup> Most WD patients have neurological symptoms, including speech disturbances, dysphagia, autonomic dysfunction, involuntary movements, and gait and balance disturbances. It was reported that associations were between neurological symptom score and increased MD in the anterior limb of the internal capsule and between a measure of disability and increased MD in frontal WM.<sup>29</sup> Shribman suggested that the association between increasing neurological severity and decreasing AD seen in chronically treated patients reflects axonal loss and WM atrophy,<sup>9</sup> which is also consistent with our findings. Our results suggest that the neurological symptoms (dysphagia, autonomic dysfunction, involuntary movements, and gait and balance disturbances) of patients with WD might be caused by demyelination in R-CST and axon involvement in L-CST (posterior part).

The corpus callosum is the largest WM bundle responsible for brain lateralization and interhemispheric communication, and the microstructural abnormalities are likely to be associated with impaired interhemispheric interactions.<sup>30</sup> Zhou and colleagues retrospectively reviewed clinical and biochemical characteristics and MRI findings of nine WD patients with corpus callosum abnormalities. Results indicated that lesions of the corpus callosum are not limited to the posterior (splenium), and that patients with corpus callosum lesions exhibited a longer course of the disease,

more severe neurological dysfunction, and more extensive brain lesions compared to WD patients with no corpus callosum lesions.<sup>31</sup> In our study, we found that MD and RD increased in CF Major (posterior part) and CF Minor, and FA decreased in the CF Major (posterior part) and CF Minor. Besides, RD values in CF Major, CF Minor showed positive correlation with UWDRS-N score. Thus, it can be demonstrated that lesions of CF are prevalent in patients of WD and correlated with clinical neurological symptoms.

Besides the regions motor, this study also observed microstructural alterations in various extra-motor areas such as the frontal areas (IFOF, CC, and UF). As frontal-temporal association fibers, previous studies indicated that they may be associated with symptoms of cognitive decline.<sup>32-34</sup> Studies focusing on neuropsychological impairments in WD have highlighted that patients with WD showing neurological signs present significant deficits in a wide range of cognitive domains.<sup>35</sup> The UF fiber links the anterior temporal lobe to the medial and lateral orbitofrontal cortex and plays a role in episodic memory, language, semantic activities, and social-emotional processing.<sup>36</sup> While IFOF may contribute to semantic processing. Damage to these fibrous microstructures may potentially correlate with cognitive impairment in patients with WD.

### Conclusion and Limitations

Some limitations of this study should be noted. First, WD is a disease with damage to both white and gray matter, while this study only evaluated lesions in the WM. In future work, we need to comprehensively evaluate the physiological mechanisms of WD disease cases, including white and gray matter, structure, and function. Because of the shortage of evaluation of cognitive function in patients with WD, we cannot assess whether lesions with interrelated WM are associated with cognitive impairment in patients.

In summary, the present study has provided evidence that the metrics of DTI could be utilized as a potential biomarker of neuro-pathological symptoms in WD. Damage to the microstructure of CF and CST may be involved in the pathophysiological process of neurological symptoms in WD patients, such as gait and balance disturbances, involuntary movements, dysphagia, and autonomic dysfunction.

**Acknowledgments.** This work was supported from the National Natural Science Foundation of China (Grant National Natural Science Foundation of China) and the University Synergy Innovation Program of Anhui Province (No. GXXT-2020-025).

**Funding.** This work was supported from the National Natural Science Foundation of China (Grant No. 81973825), the Anhui Provincial Natural Science Foundation of China (Grant No. 2108085QH367), the Open Fund Project of Key Laboratory of Xin'An Medicine of Ministry of Education (No. 2020xayx12), and the University Synergy Innovation Program of Anhui Province (No. GXXT-2020-025).

**Conflicts of Interest.** The authors declare that there is no conflict of interest regarding the publication of this paper.

**Author Contributions.** T.H.W., Y.L.Y., Y.F.D., and C.F.Z. have contributed to the collection of experimental data. H.L.W. and Y.W. have contributed to data analysis.

## References

- Bhattacharya K, Thankappan B. Wilson's disease update: an Indian perspective. *Ann Indian Acad Neurol.* 2022;25:43–53. DOI [10.4103/aian.aian\\_1070\\_21](https://doi.org/10.4103/aian.aian_1070_21).
- Shribman S, Warner TT, Dooley JS. Clinical presentations of Wilson disease. *Ann Transl Med.* 2019;7:S60–S60. DOI [10.21037/atm.2019.04.27](https://doi.org/10.21037/atm.2019.04.27).
- Hu S, Xu C, Dong T, et al. Structural and functional changes are related to cognitive status in Wilson's disease. *Front Hum Neurosci.* 2021;15:610947. DOI [10.3389/fnhum.2021.610947](https://doi.org/10.3389/fnhum.2021.610947).
- Wang RM, Yu H, Yang GM, et al. Clinical features and outcome of Wilson's disease with generalized epilepsy in Chinese patients. *CNS Neurosci Ther.* 2020;26:842–50. DOI [10.1111/cns.13373](https://doi.org/10.1111/cns.13373).
- Tang S, Bai L, Hou W, et al. Comparison of the effectiveness and safety of d-penicillamine and zinc salt treatment for symptomatic Wilson disease: a systematic review and meta-analysis. *Front Pharmacol.* 2022;13:847436. DOI [10.3389/fphar.2022.847436](https://doi.org/10.3389/fphar.2022.847436).
- Redzia-Ogrodnik B, Czlonkowska A, Bembek J, et al. Brain magnetic resonance imaging and severity of neurological disease in Wilson's disease - the neuroradiological correlations. *Neurol Sci.* 2022;43:4405–4412. DOI [10.1007/s10072-022-06001-2](https://doi.org/10.1007/s10072-022-06001-2).
- Song Y, Zou L, Zhao J, et al. Whole brain volume and cortical thickness abnormalities in Wilson's disease: a clinical correlation study. *Brain Imaging Behav.* 2021;15:1778–87. DOI [10.1007/s11682-020-00373-9](https://doi.org/10.1007/s11682-020-00373-9).
- Li G, Zhou X, Xu P, Pan X, Chen Y. Microstructure assessment of the thalamus in Wilson's disease using diffusion tensor imaging. *Clin Radiol.* 2014;69:294–8. DOI [10.1016/j.crad.2013.10.016](https://doi.org/10.1016/j.crad.2013.10.016).
- Shribman S, Bocchetta M, Sudre CH, et al. Neuroimaging correlates of brain injury in Wilson's disease: a multimodal, whole-brain MRI study. *Brain.* 2022;145:263–75. DOI [10.1093/brain/awab274](https://doi.org/10.1093/brain/awab274).
- Carbine KA, Duraccio KM, Hedges-Muncy A, Barnett KA, Kirwan CB, Jensen CD. White matter integrity disparities between normal-weight and overweight/obese adolescents: an automated fiber quantification tractography study. *Brain Imaging Behav.* 2020;14:308–19. DOI [10.1007/s11682-019-00036-4](https://doi.org/10.1007/s11682-019-00036-4).
- Qu Y, Wang P, Liu B, et al. Altered connection and diagnosis utility of white matter in Alzheimer's disease: a multi-site automated fiber quantification study. *Annu Int Conf IEEE Eng Med Biol Soc.* vol. 2021, 2021, pp. 2923–7, DOI [10.1109/EMBC46164.2021.9630117](https://doi.org/10.1109/EMBC46164.2021.9630117)
- Deng X, Yin H, Zhang Y, et al. Impairment and plasticity of language-related white matter in patients with brain arteriovenous malformations. *Stroke.* 2021, STROKEAHA121035506. DOI [10.1161/STROKEAHA.121.035506](https://doi.org/10.1161/STROKEAHA.121.035506).
- Li R, Sun H, Hao H, et al. White matter integrity in patients with classic trigeminal neuralgia: a multi-node automated fiber tract quantification study. *J Int Med Res.* 2021;49:3000605211047071. DOI [10.1177/03000605211047071](https://doi.org/10.1177/03000605211047071).
- European Association for Study of Liver. EASL Clinical Practice Guidelines: Wilson's disease. *J Hepatol.* 2012;56:671–85. DOI [10.1016/j.jhep.2011.11.007](https://doi.org/10.1016/j.jhep.2011.11.007).
- Wang A, Wu H, Xu C, et al. Study on lesion assessment of cerebello-thalamo-cortical network in Wilson's disease with diffusion tensor imaging. *Neural Plast.* 2017;2017:7323121. DOI [10.1155/2017/7323121](https://doi.org/10.1155/2017/7323121).
- Czlonkowska A, Tarnacka B, Moller JC, et al. Unified Wilson's disease rating scale - a proposal for the neurological scoring of Wilson's disease patients. *Neurol Neurochir Pol.* 2007;41:1–12. DOI [doi](https://doi.org/10.1016/j.jhep.2011.11.007).
- Yeatman JD, Dougherty RF, Myall NJ, Wandell BA, Feldman HM, Beaulieu C. Tract profiles of white matter properties: automating fiber-tract quantification. *PLoS One.* 2012;7:e49790. DOI [10.1371/journal.pone.0049790](https://doi.org/10.1371/journal.pone.0049790).
- Dusek P, Lescinskij A, Ruzicka F, et al. Associations of brain atrophy and cerebral iron accumulation at MRI with clinical severity in Wilson disease. *Radiology.* 2021;299:662–72. DOI [10.1148/radiol.2021202846](https://doi.org/10.1148/radiol.2021202846).
- Zou L, Song Y, Zhou X, Chu J, Tang X. Regional morphometric abnormalities and clinical relevance in Wilson's disease. *Mov Disord.* 2019;34:545–54. DOI [10.1002/mds.27641](https://doi.org/10.1002/mds.27641).
- Zhou XX, Li XH, Chen DB, et al. The asymmetry of neural symptoms in Wilson's disease patients detecting by diffusion tensor imaging, resting-state functional MRI, and susceptibility-weighted imaging. *Brain Behav.* 2018;8:e00930. DOI [10.1002/brb3.930](https://doi.org/10.1002/brb3.930).
- Morava E, Baumgartner M, Patterson M, Rahman S, Zschocke J, Peters V. Improvement of Diffusion Tensor Imaging (DTI) parameters with decoppering treatment in Wilson's disease. *JIMD Rep.* 2016;25:31–7. DOI [10.1007/8904\\_2015\\_466](https://doi.org/10.1007/8904_2015_466).
- Shu M, Yu C, Shi Q, et al. Alterations in white matter integrity and asymmetry in patients with benign childhood epilepsy with centrotemporal spikes and childhood absence epilepsy: an automated fiber quantification tractography study. *Epilepsy Behav.* 2021;123:108235. DOI [10.1016/j.yebeh.2021.108235](https://doi.org/10.1016/j.yebeh.2021.108235).
- Stone DB, Ryman SG, Hartman AP, et al. Specific white matter tracts and diffusion properties predict conversion from mild cognitive impairment to Alzheimer's disease. *Front Aging Neurosci.* 2021;13:711579. DOI [10.3389/fnagi.2021.711579](https://doi.org/10.3389/fnagi.2021.711579).
- Kalita J, Kumar V, Parashar V, Misra UK. Neuropsychiatric manifestations of Wilson disease: correlation with MRI and glutamate excitotoxicity. *Mol Neurobiol.* 2021;58:6020–31. DOI [10.1007/s12035-021-02525-4](https://doi.org/10.1007/s12035-021-02525-4).
- Bastin ME, Pettit LD, Bak TH, Gillingwater TH, Smith C, Abrahams S. Quantitative tractography and tract shape modeling in amyotrophic lateral sclerosis. *J Magn Reson Imaging.* 2013;38:1140–5. DOI [10.1002/jmri.24073](https://doi.org/10.1002/jmri.24073).
- Schulz R, Koch P, Zimmerman M, et al. Parietofrontal motor pathways and their association with motor function after stroke. *Brain.* 2015;138:1949–60. DOI [10.1093/brain/aww100](https://doi.org/10.1093/brain/aww100).
- Schulz R, Park C-H, Boudrias M-H, Gerloff C, Hummel FC, Ward NS. Assessing the integrity of corticospinal pathways from primary and secondary cortical motor areas after stroke. *Stroke.* 2012;43:2248–51. DOI [10.1161/STROKEAHA.112.662619](https://doi.org/10.1161/STROKEAHA.112.662619).
- Vuong A, Fowler EG, Matsumoto J, Staudt LA, Yokota H, Joshi SH. Selective motor control is a clinical correlate of brain motor tract impairment in children with spastic bilateral cerebral palsy. *AJNR Am J Neuroradiol.* 2021;42:2054–61. DOI [10.3174/ajnr.A7272](https://doi.org/10.3174/ajnr.A7272).
- Jadav R, Saini J, Sinha S, Bagepally B, Rao S, Taly AB. Diffusion tensor imaging (DTI) and its clinical correlates in drug naive Wilson's disease. *Metab Brain Dis.* 2013;28:455–62. DOI [10.1007/s11011-013-9407-1](https://doi.org/10.1007/s11011-013-9407-1).
- Lin Q, Bu X, Wang M, et al. Aberrant white matter properties of the callosal tracts implicated in girls with attention-deficit/hyperactivity disorder. *Brain Imaging Behav.* 2020;14:728–35. DOI [10.1007/s11682-018-0010-2](https://doi.org/10.1007/s11682-018-0010-2).



31. Zhou ZH, Wu YF, Cao J, et al. Characteristics of neurological Wilson's disease with corpus callosum abnormalities. *BMC Neurol.* 2019;19:85. DOI [10.1186/s12883-019-1313-7](https://doi.org/10.1186/s12883-019-1313-7).
32. Jiang Y, Liu Y, Gao B, et al. Segmental abnormalities of white matter microstructure in end-stage renal disease patients: an automated fiber quantification tractography study. *Front Neurosci.* 2021;15:765677. DOI [10.3389/fnins.2021.765677](https://doi.org/10.3389/fnins.2021.765677).
33. Huang L, Chen X, Sun W, et al. Early segmental white matter fascicle microstructural damage predicts the corresponding cognitive domain impairment in cerebral small vessel disease patients by automated fiber quantification. *Front Aging Neurosci.* 2020;12:598242. DOI [10.3389/fnagi.2020.598242](https://doi.org/10.3389/fnagi.2020.598242).
34. Unterrainer HF, Hiebler-Ragger M, Koschutnig K, et al. Brain structure alterations in poly-drug use: reduced cortical thickness and white matter impairments in regions associated with affective, cognitive, and motor functions. *Front Psychiatry.* 2019;10:667. DOI [10.3389/fpsyt.2019.00667](https://doi.org/10.3389/fpsyt.2019.00667).
35. Peyroux E, Santaella N, Broussolle E, et al. Social cognition in Wilson's disease: a new phenotype? *PLoS One.* 2017;12:e0173467. DOI [10.1371/journal.pone.0173467](https://doi.org/10.1371/journal.pone.0173467).
36. Zekelman LR, Zhang F, Makris N, et al. White matter association tracts underlying language and theory of mind: an investigation of 809 brains from the Human Connectome Project. *Neuroimage.* 2022;246:118739. DOI [10.1016/j.neuroimage.2021.118739](https://doi.org/10.1016/j.neuroimage.2021.118739).